Gene Expression Changes during the Development of Acute Lung Injury

Role of Transforming Growth Factor β

Scott C. Wesselkamper, Lisa M. Case, Lisa N. Henning, Michael T. Borchers, Jay W. Tichelaar, John M. Mason, Nadine Dragin, Mario Medvedovic, Maureen A. Sartor, Craig R. Tomlinson, and George D. Leikauf

Department of Environmental Health, Center for Environmental Genetics, and Division of Pulmonary and Critical Care Medicine, Department of Internal Medicine, University of Cincinnati Medical Center, University of Cincinnati, Cincinnati, Ohio

Rationale: **Acute lung injury can occur from multiple causes, resulting in high mortality. The pathophysiology of nickel-induced acute lung injury in mice is remarkably complex, and the molecular mechanisms are uncertain.**

Objectives: **To integrate molecular pathways and investigate the role of transforming growth factor β (TGF-β) in acute lung injury in mice.**

Methods: **cDNA microarray analyses were used to identify lung gene expression changes after nickel exposure. MAPPFinder analysis of the microarray data was used to determine significantly altered molecular pathways. TGF-β1 protein in bronchoalveolar lavage fluid, as well as the effect of inhibition of TGF-β, was assessed in nickel-exposed mice. The effect of TGF-β on surfactant-associated protein B (*Sftpb*) promoter activity was measured in mouse lung epithelial cells.**

Measurements and Main Results: **Genes that decreased the most after nickel exposure play important roles in lung fluid absorption or surfactant and phospholipid synthesis, and genes that increased the most were involved in TGF-β signaling. MAPPFinder analysis further established TGF-β signaling to be significantly altered. TGF-β–inducible genes involved in the regulation of extracellular matrix function and fibrinolysis were significantly increased after nickel exposure, and TGF-β1 protein was also increased in the lavage fluid. Pharmacologic inhibition of TGF-β attenuated nickel-induced protein in bronchoalveolar lavage. In addition, treatment with TGF-β1 dose-dependently repressed *Sftpb* promoter activity *in vitro*, and a novel TGF-β–responsive region in the *Sftpb* promoter was identified.**

Conclusions: **These data suggest that TGF-β acts as a central mediator of acute lung injury through the alteration of several different molecular pathways.**

Keywords: microarray; surfactant; fibrinolysis; extracellular matrix

Acute lung injury is common in critically ill patients and results from a variety of factors, including pneumonia, sepsis, trauma, and inhaled irritants (1). Acute lung injury involves epithelial and endothelial damage that subsequently leads to impairment of alveolar fluid clearance (edema), alveolar hemorrhage, disruption of surfactant homeostasis, degeneration of the alveolar capillary–epithelial barrier, and inadequate gas exchange (2). The prognosis for survival from acute lung injury is poor, with mortality at 20 to 40%; and, if resolution occurs, persistent pulmonary complications develop, including interstitial fibrosis and diminished lung compliance.

Transforming growth factor β (TGF-β) exists in three isoforms and is a member of a family of growth factors that is able to modulate several cellular processes in multiple organ systems (3). Of these isoforms, TGF-β1 is generated in greatest abundance subsequent to tissue damage (4). TGF-β has been widely studied for its vital role in the development of fibrosis after injury to the lung (5, 6). A broader function for TGF-β is suggested from evidence that elevated levels of TGF-β1 (as well as TGF-β–inducible genes, such as procollagen, type III, α1) have been demonstrated in the lungs of patients with acute respiratory distress syndrome (7–9). Furthermore, in mouse models of bleomycin-induced lung injury, TGF-β–inducible genes are increased within 48 h (10). Although the underlying mechanisms of TGF-β mediation of acute lung injury are uncertain, studies have shown that TGF-β may augment pulmonary injury through increased endothelial (11) and epithelial permeability (12) and decreased ion and fluid transport (13–15). These data suggest that TGF-β may have a role in the development of acute lung injury in addition to the regulation of fibroproliferation.

Prior studies from our laboratory have assessed aspects of the molecular mechanisms involved in the pathogenesis of acute lung injury using inhaled nickel in mice (16–18). The purpose of our study was to use oligonucleotide microarray analysis to identify novel intersecting molecular pathways that lead to the development of acute lung injury. The TGF-β signaling pathway was identified as being significantly altered in our mouse model of nickel-induced acute lung injury by means of initial application of general microarray statistical analysis, as well as the MAPPFinder analytic tool that creates a global gene expression profile at the level of biological processes (19). Consistent with this, TGF-β1 protein levels were significantly increased in the bronchoalveolar lavage fluid (BALF) of mice after 72 h of nickel exposure. We also identified expression changes in TGF-β–responsive genes involved in extracellular matrix changes, fibrinolysis, and surfactant synthesis. Pharmacologic inhibition of TGF-β with soluble chimeric TGF-β type II receptor–IgG-Fc (TGFβRII-Fc) attenuated nickel-induced protein in BAL. Using promoter deletion constructs transiently transfected into mouse lung epithelial cells, we identified a novel TGF-β regulatory region in the mouse surfactant-associated protein B (*Sftpb*) promoter. Taken together, these data suggest TGF-β is a central mediator of acute lung injury.

METHODS

Mice and Exposure Protocol

Female 129S1/SvImJ mice (age, 7–10 wk) were purchased from the Jackson Laboratory (Bar Harbor, ME), and housed in our animal facilities 1 wk or more before exposure. Nickel aerosol was generated from a 50-mM solution of $NiSO_4 \cdot 6\ H_2O$ (Sigma, St. Louis, MO) and monitored as described previously (16). Mice were exposed for 3 to 72 h to

(*Received in original form February 22, 2005; accepted in final form August 9, 2005*)

Supported by National Institutes of Health grants ES10562, HL65612, ES06096, and ES07250.

Correspondence and requests for reprints should be addressed to George D. Leikauf, Ph.D., Department of Environmental Health, P.O. Box 670056, University of Cincinnati, Cincinnati, OH 45267-0056. E-mail: george.leikauf@uc.edu

Am J Respir Crit Care Med Vol 172. pp 1399–1411, 2005
Originally Published in Press as DOI: 10.1164/rccm.200502-286OC on August 11, 2005
Internet address: www.atsjournals.org

150 ± 15 μg Ni^{2+}/m^3 in a 0.32-m^3 stainless steel inhalation chamber. All experimental protocols were reviewed and approved by the Institutional Animal Care and Use Committee at the University of Cincinnati Medical Center.

Lung Tissue Preparation and RNA Isolation

After exposure, mice were killed with an intraperitoneal injection of 50 mg/kg of sodium pentobarbital followed by exsanguination. Lungs were removed, placed in liquid nitrogen, and stored at −80°C. Total cellular RNA was isolated from frozen lung tissue with Trizol (Invitrogen, Carlsbad, CA), and quantity was assessed by A260/A280 spectrophotometric absorbance (SmartSpec 3000; Bio-Rad, Hercules, CA).

For gross pathologic analysis, the trachea was ligated, and the entire heart-lung block was removed from the chest cavity, washed with phosphate-buffered saline, and digitally photographed. To examine lung pathology, the diaphragm was punctured, a cannula was inserted into the trachea, and the lungs were instilled *in situ* with phosphate-buffered formalin (∼ 900 μl, pH 7.1; Fisher Scientific, Fairlawn, NJ). After fixation, lung tissue was dehydrated, processed into paraffin blocks, sagittally sectioned (5 μm), and stained with hematoxylin and eosin.

RNA Expression Analysis by Oligonucleotide Microarray and Reverse Transcriptase–Polymerase Chain Reaction

Lung RNA quality was assessed by separation with a denaturing formaldehyde/agarose/ethidium bromide gel, and quantified by analysis with an Agilent Bioanalyzer (Quantum Analytics, Inc., Foster City, CA). To examine differential gene expression of 13,443 70-mer oligonucleotides, a microarray was fabricated by the Genomic and Microarray Laboratory, Center for Environmental Genetics, University of Cincinnati (http://microarray.uc.edu/), using a commercial library (Qiagen-Operon, Alameda, CA). Clones (70-mers) from the Operon Library were amplified by polymerase chain reaction (PCR), printed onto glass slides (Omnigrid Microarrayer; GeneMachines, San Carlos, CA), and consisted of 8,077 known genes: 5,017 RIKEN cDNAs, 210 nonannotated sequences/segments/IMAGE clones, and 139 genes for hypothetical proteins. Exposure groups consisted of nine mice. RNA from three mice per group were pooled for each microarray, and three separate microarrays per exposure group were compared with nonexposed control animals using 20 μg total RNA per array. Each sample of mRNA was reverse transcribed and randomly reciprocally tagged with fluorescent cyanine 3 (Cy3) or cyanine 5 (Cy5; e.g., Cy3 for control and Cy5 for 72-h exposure). Cy3 and Cy5 samples were cohybridized with the printed 70-mers. After hybridization, slides were washed and scanned at 635 (Cy5) and 532 (Cy3) nm (GenePix 4000B; Axon Instruments, Inc., Union City, CA). Data normalization was performed in three steps for each microarray as described previously (20). Consistency of fluorescence measurements in different hybridizations was assessed by calculating pairwise correlation coefficients between measurements for the same mouse in different hybridizations. Pairwise Pearson's correlation coefficients were above 0.9, indicating the reproducibility of measurements.

To further assess the expression changes of genes within the TGF-β and fibrinolysis molecular pathways in lungs of mice exposed to nickel for 24, 48, and 72 h, as well as nonexposed control animals, reverse transcriptase–PCR (RT-PCR) was performed (SingleGene PCR kits; SuperArray, Frederick, MD). Initially, reverse transcription reactions were performed with 2.5 μg of total RNA (First Strand cDNA synthesis kit; SuperArray), and the reactions were stored at −20°C. PCR reactions used manufacturer-supplied primer pairs to measure the following: integrin αV (*Itgav*; cat. no. SPM-0796A, 24 cycles, 559-bp product); secreted phosphoprotein 1 (*Spp1*; cat. no. SPM-0782A, 24 cycles, 567-bp product); TGF-β1 (*Tgfb1*; cat. no. SPM-0112A, 24 cycles, 463-bp product); thrombospondin 1 (*Thbs1*; cat. no. SPM-0221A, 32 cycles, 443-bp product); tenascin C (*Tnc*; cat. no. SPM-0945A, 30 cycles, 480-bp product); and serine (or cysteine) proteinase inhibitor, clade E, member 1 (*Serpine1*; cat. no. SPM-0216A, 24 cycles, 470-bp product). The expression levels of these genes were normalized to the expression of the ribosomal protein S2 (*Rps2*; cat. no. SPM-0479A, 24 cycles, 423-bp product). Data acquisition was performed by electrophoresis of 10 μl of each reaction on a 2% agarose gel containing 0.5 μg/ml ethidium bromide, and band intensities were analyzed with a Typhoon 8600 imager and ImageQuant software (Amersham Biosciences, Piscataway, NJ).

BAL and TGF-β1 Immunoassay

To measure TGF-β protein levels in the lung, BALF was collected from mice (n = 5) exposed for 72 h and compared with nonexposed control animals (n = 5). Mice were anesthetized, the diaphragm punctured, and the lungs were lavaged with two 1-ml aliquots of Hanks' balanced salt solution without Ca^{2+} and Mg^{2+} (pH 7.2, 37°C; Invitrogen). Recovered BALF samples were centrifuged ($500 \times g$, 5 min, 4°C), and the cell-free supernatants were decanted and stored at −80°C until concentrated with centrifugal filter devices (Microcon YM-3; Millipore, Bedford, MA). To determine the concentration of TGF-β1 in BAL supernatants, an ELISA assay (Quantikine, cat. no. MB100; R&D Systems, Minneapolis, MN) was used according to the manufacturer's protocol. The lower limit of detection for TGF-β1 was 2.9 pg/ml.

Inhibition of TGF-β *In Vivo*

Murine soluble chimeric TGFβRII-Fc (Biogen Idec, Cambridge, MA; 50 μg in 50 μl sterile saline) or saline alone was intravenously administered to 129S1/SvImJ mice immediately before and 6 and 30 h after a 24-h exposure to nickel (n = 5 mice/group). Nonexposed control mice were concurrently injected with saline (n = 5). All mice were lavaged 72 h after the initiation of nickel exposure as previously described. Aliquots (200 μl) of BALF were cytocentrifuged (Cytospin; Shandon Scientific Ltd., Runcorn, United Kingdom), and the cells were stained with Hemacolor (EM Science, Gibbstown, NJ) for differential cell analysis. Differential cell counts were performed according to standard cytologic procedures by identifying at least 300 cells (21). Total cell counts were performed with a hemacytometer using trypan blue (Invitrogen). Total BAL protein was measured in cell-free supernatants using a bicinchoninic acid assay with bovine serum albumin used as the standard (Pierce, Rockford, IL).

Mouse Lung Epithelial Cell Culture, Transfections, and Reporter Gene Assay

To investigate the effect of TGF-β on *Sftpb* transcription, mouse lung epithelial (MLE)-15 cells were grown in HITES (hydrocortisone, insulin, transferrin, estradiol, and sodium selenite) medium containing 4% fetal bovine serum (Sigma), as previously described (22), and transfected with *Sftpb* promoter constructs. These constructs were cloned in pGL3-basic luciferase reporter vector (Promega, Madison, WI) and sequenced. The initial promoter *Sftpb* template was a DNA sequence that contained 653 bp (−653) 5′ and 35 bp (+35) 3′ to the transcriptional start site. Using the –653/+35 (wild-type) *Sftpb* construct as a template, a Δ(−616/−198) promoter deletion construct was generated using *Pvu*II and *Bpu10*I restriction endonuclease sites followed by blunt-end ligations. Transient transfections were conducted using FuGENE 6 transfection reagent (3 μl/well; Roche Applied Science, Indianapolis, IN), as per the manufacturer's instructions, in six-well Costar plates in duplicate or triplicate samples on at least two occasions. The *Sftpb* promoter constructs (750 ng/well) were cotransfected with cytomegalovirus promotor–β-galactosidase (250 ng/well) as an internal transfection control. Transfected MLE-15 cells were treated with 0, 1.0, 10, and 30 ng/ml TGF-β1 (R&D Systems; cat. no. 240-B) for 24 h. Cell extracts were prepared with one freeze–thaw cycle in 200 μl Reporter lysis buffer (Promega). Luciferase assays were performed using the Luciferase Assay System (Promega), and relative luciferase units for each sample were measured in a single-tube luminometer (Sirius; Berthold Detection Systems, Oak Ridge, TN). β-Galactosidase activity for each sample was measured in 96-well Falcon plates using the β-galactosidase Enzyme Assay System (Promega) and a Spectramax Plus spectrophotometer (Molecular Devices, Sunnyvale, CA). All relative luciferase unit measurements were normalized to β-galactosidase values.

Statistical Analysis and Assessment of Microarray Data

Statistical analysis of microarray data was performed by fitting the following mixed-effects linear model for each gene separately: $Y_{ijk} = m + A_i + S_j + C_k + e_{ijk}$, where the Y_{ijk} corresponds to the normalized log-intensity on the i^{th} array (i = 1,...,48), labeled with the k^{th} dye (k = 1 for Cy5 and k = 2 for Cy3) and for the j^{th} treatment condition, and m is

the overall mean log-intensity, A_i is the effect of the i^{th} array, S_j is the effect of the j^{th} treatment condition, and C_k is the effect of the k^{th} dye. Assumptions about model parameters were the same as described by Wolfinger and colleagues (23), with array effects assumed to be random, and treatment and dye effects assumed to be fixed. This model was fitted for each gene, and statistical significance of the differential expression between exposure groups after adjusting for the array and dye effects was assessed by calculating p values for corresponding linear contrasts. Multiple hypotheses testing adjustment was performed by calculating a false discovery rate (FDR) (24), and comparisons of the effect of various stringencies for statistical significance were performed. The data normalization and the statistical analysis were performed using SAS statistical software package (SAS Institute, Inc., Cary, NC). Each treatment comparison was performed in triplicate, and the data discussed in this article were analyzed as part of a larger experiment that involved two earlier time points of nickel exposure, as well as equivalent time series in two different mouse strains.

To further analyze the microarray dataset, we used the MAPPFinder program to dynamically link microarray data to the Gene Ontology (GO) hierarchy database as illustrated previously (19). MAPPFinder generates a gene expression profile at the level of biological processes, cellular components, and molecular functions that allows for identification of specific biological pathways that merit further investigation. The results, calculated using Fisher's exact test, are expressed as a "z score" for a particular pathway, and values greater than 2.0 were considered to be significant. GenMAPP was also used to view and analyze microarray data on biological pathways (25).

RT-PCR quantitation data, TGF-β1 immunoassay data, BAL data, and *Sftpb* reporter construct data are presented as means ± SEM. Significant differences among groups were identified by analysis of variance. Individual comparisons between groups were confirmed by the two-tailed Student's *t* test. A p value less than 0.05 was considered statistically significant.

RESULTS

Identification of Transcriptional Changes during Acute Lung Injury

After exposure to nickel, lung mRNA expression of 129S1/SvImJ mice was analyzed using oligonucleotide microarrays at various times. Of the 13,664 genes that were present on the array, 77% or more were detected in each array. For the purposes of this analysis, we only considered values significantly different from control values when p was less than 0.5 times 10^{-6}, expected false-positive factor was less than 0.05, and the FDR was less than 0.0003, with an average intensity of at least 300, ensuring a high degree of confidence in the identified genes. Genes with the greatest decreases in expression are presented in Table 1, and are sorted by their 72-h mean expression value. Twenty-one of the 26 genes listed in Table 1 are localized to the lung, and eight are expressed in alveolar type II cells. The molecular functions of these genes as classified by GO are varied. Several of these genes with significantly decreased expression play important roles in fluid absorption and the synthesis, trafficking, or reutilization of surfactant proteins and phospholipids. These genes include ATPase, Na^+/K^+ transporting, β1 polypeptide (*Atp1b1*), solute carrier family 34 (sodium phosphate), member 2 (*Slc34a2*), carbonyl reductase 2 (*Cbr2*), fatty acid synthase (*Fasn*), napsin A aspartic peptidase (*Napsa*), stearoyl-coenzyme A desaturase 2 (*Scd2*), and phospholipid transfer protein (*Pltp*). Expression of a related gene, sodium channel, nonvoltage-gated 1β (*Scnn1b*), was also decreased –1.9 ± 0.4-fold, and although likely significant (FDR = 0.01; p = 0.0008), it did not reach the twofold threshold for inclusion. Thus, downregulation of these genes may result in disruption of essential lung surfactant function and alveolar fluid clearance in our model of nickel-induced acute lung injury.

Genes with the greatest increases in expression during nickel-induced acute lung injury are presented in Table 2, and are also sorted by their 72-h mean expression value. Of the 32 genes listed in Table 2, 28 were previously detected in lung, and a subset of these 28 included 16 that were detected in alveolar type II cells. The GO molecular functions of the genes with increasing expression were again wideranging. Notably, a number of the genes with significantly increased expression are known to be regulated by TGF-β signaling, including *Thbs1*, S100 calcium-binding protein A9 (calgranulin B; *S100a9*), *Tnc*, *Spp1*(also known as osteopontin), *Serpine1* (also known as plasminogen activator inhibitor-1 [*PAI-1*]), and matrix metalloproteinase 14 (membrane-inserted; *Mmp14*). These changes suggest that activation of the TGF-β pathway could be an important molecular event in the development of nickel-induced acute lung injury.

To further evaluate our microarray data, GenMAPP and MAPPFinder were used to organize gene expression data into MAPPs (microarray pathway profiles) that represent specific biological pathways and functionally grouped genes. We focused on microarray gene expression data from mice exposed for 72 h. Using gene-association files from the GO Consortium, MAPPFinder assigns the thousands of genes in the 72-h expression dataset to numerous GO terms. Several significant (i.e., z score > 2.0) functional MAPPs were revealed with MAPPFinder and are presented in Table 3. Consistent with our initial assessment above, the TGF-β signaling pathway was significantly changed at 72 h (z score = 2.8), reinforcing the importance of this pathway in our model of acute lung injury. Gene pathways that are involved in processes of the extracellular matrix (e.g., proteolysis, fibrinolysis; z score = 3.7) and cytokine and chemokine production (z scores = 2.8 and 2.3, respectively) are also significantly changed.

Activation of the TGF-β Signaling Pathway during Acute Lung Injury

The amount of TGF-β1 protein released in the lung during nickel-induced acute lung injury was assessed in the BALF by an immunoassay for TGF-β1. TGF-β1 increased in 72-h nickel-exposed mice as compared with control animals (Figure 1). The transcript levels of TGFB1 also were increased significantly over nonexposed control values after 72 h as measured by RT-PCR (1.9 ± 0.2-fold, $p < 0.05$). These results agree with the increased gene expression of genes known to activate TGF-β (i.e., *Itgav* and *Thbs1*) shown in Figure 2B.

An overview of expression changes in the TGF-β pathway are presented in Figure 2A for 129S1/SvImJ mice exposed to nickel for 72 h. To visually analyze the TGF-β signaling pathway, GenMAPP was used to characterize the response at 72 h. Increases and decreases in gene expression are presented as fold changes as compared with nonexposed control mice. Of the 38 genes examined in the TGF-β pathway, 21 were significantly altered, with 16 increased (shown in *red*) and 5 decreased (shown in *green*). The increases in expression were mostly in genes known to stimulate the pathway, and the decreases were in genes known to inhibit the pathway. Thus, these changes are consistent with activation of TGF-β signaling.

RT-PCR was performed using SuperArray SingleGene PCR kits to confirm the expression changes of key genes in this pathway. Increases in expression of genes that are activators of TGF-β (*Itgav* and *Thbs1*; Figure 2B), and genes that are activated by TGF-β (*Spp1*, tissue inhibitor of metalloproteinase 1 [*Timp1*], and *Tnc*; Figure 2C) after 24, 48, and 72 h of nickel exposure were confirmed.

Modulation of the Fibrinolysis Cascade during Acute Lung Injury

The involvement of fibrinolysis and coagulation in our model of nickel-induced acute lung injury was also evaluated on gross

TABLE 1. SIGNIFICANTLY DECREASED GENES DETERMINED BY OLIGONUCLEOTIDE MICROARRAY ANALYSIS IN 129S1/SVIMJ MOUSE LUNGS AFTER EXPOSURE TO NICKEL FOR 24, 48, OR 72 H

Accession ID	Name	Symbol	Intensity	24 h	SEM	48 h	SEM	72 h	SEM	Molecular Function‡
M77497	Cytochrome P450, family 2, subfamily f, polypeptide 2*	Cyp2f2	9,775	−5.0	1.1	−7.9	1.7	−31.4	6.8	Monooxygenase activity
X61433	**ATPase, Na+/K+ transporting, β1 polypeptide†**	**Atp1b1**	**719**	**−4.7**	**1.2**	**−7.9**	**2.0**	**−25.7**	**7.8**	**Na^+/K^+-exchanging ATPase activation**
AF081499	**Solute carrier family 34 (sodium phosphate), member 2†**	**Slc34a2**	**1,615**	**−7.1**	**1.9**	**−6.5**	**1.7**	**−7.7**	**2.0**	**Na^+-dependent phosphate transporter activation**
M21856	Cytochrome P450, family 2, subfamily b, polypeptide 10†	Cyp2b10	864	−2.7	0.5	−6.6	1.3	−6.8	1.3	Monooxygenase activity
D26123	**Carbonyl reductase 2†**	**Cbr2**	**31,940**	**−1.7**	**0.3**	**−3.8**	**0.6**	**−6.5**	**1.1**	**Carbonyl reductase (NADPH) activity**
V00722	Hemoglobin, β adult minor chain	Hbb-b2	15,666	−1.3	0.4	−3.6	1.0	−5.3	1.4	Oxygen transporter activity
X55663	Cytoplasmic tyrosine kinase, Dscr28C-related (*Drosophila*)*	Tec	1,476	−2.2	0.5	−4.5	1.0	−5.1	1.2	Kinase activity
NM_026352	Peptidylprolyl isomerase D (cyclophilin D)*	Ppid	983	−2.1	0.5	−5.2	1.4	−5.0	1.3	Peptidyl-prolyl cis-trans isomerase activity
NM_031180	Klotho β*	Klb	1,375	−3.6	0.5	−2.5	0.4	−4.9	0.7	Hydrolase activity, hydrolyzing O-glycosyl compounds
M96823	Nucleobindin	Nucb	25,358	−1.0	0.2	−2.8	0.6	−4.7	1.0	DNA binding
M18776	Microtubule-associated protein τ*	Mapt	519	−1.3	0.3	−2.2	0.5	−4.7	1.1	Cytoskeletal regulatory protein binding
X13135	**Fatty acid synthase†**	**Fasn**	**418**	**−3.0**	**0.8**	**−5.0**	**1.3**	**−4.6**	**1.1**	**Fatty acid synthase activity**
U72031	Eosinophil-associated, RNase A family, member 2*	Ear2	359	−1.4	0.3	−2.4	0.5	−4.4	0.9	Endonuclease activity
NM_023624	Lecithin-retinol acyltransferase*	Lrat	316	−1.7	0.5	−1.2	0.3	−4.4	1.2	O-acyltransferase activity
NM_028288	Cullin 4B	Cul4b	484	−2.4	0.5	−3.4	0.7	−4.3	0.9	(Protein binding/ubiquitin ligase)
NM_010000	Cytochrome P450, family 2, subfamily b, polypeptide 9†	Cyp2b9	622	−2.3	0.7	−4.7	1.3	−4.3	1.2	Monooxygenase activity
U29875	FMS-like tyrosine kinase 3 ligand	Flt3l	305	−2.4	0.7	−3.2	0.9	−4.2	1.2	Kinase activity
AB038144	**Napsin A aspartic peptidase†**	**Napsa**	**1,229**	**−2.5**	**0.6**	**−4.4**	**1.0**	**−4.0**	**0.9**	**Pepsin A activity**
M26270	**Stearoyl-coenzyme A desaturase 2†**	**Scd2**	**4,284**	**−2.3**	**0.4**	**−1.9**	**0.3**	**−3.6**	**0.6**	**Stearoyl-CoA 9-desaturase activity**
Y08135	Sphingomyelin phosphodiesterase, acidlike 3A	Smpdl3a	430	−1.7	0.4	−1.7	0.4	−3.6	0.8	Hydrolase activity, acting on glycosyl bonds
AF230074	Iroquois-related homeobox 5 (*Drosophila*)*	Irx5	375	−2.1	0.5	−2.5	0.6	−3.3	0.8	Transcription factor activity
AK010249	Procollagen C-endopeptidase enhancer 2*	Pcolce2	1,020	−1.9	0.5	−2.2	0.5	−3.2	0.8	(Protein binding)
U37226	**Phospholipid transfer protein†**	**Pltp**	**760**	**−1.8**	**0.4**	**−2.9**	**0.7**	**−3.1**	**0.7**	**Lipid binding**
NM_020510	Frizzled homolog 2 (*Drosophila*)*	Fzd2	497	−2.4	0.3	−2.1	0.3	−3.1	0.4	G-protein–coupled receptor activity
M15501	Actin, α, cardiac*	Actc1	2,127	1.0	0.2	−1.8	0.3	−3.1	0.5	Motor activity
X81584	Insulinlike growth factor binding protein 6*	Igfbp6	4,496	−1.6	0.3	−2.3	0.4	−3.1	0.5	Insulinlike growth factor binding

Values shown for each time point are mean fold changes below nonexposed control values. Genes are sorted by 72-h mean value and were considered statistically significant if intensity > 300, $p < 0.5 \times 10^{-6}$, expected false-positive factor < 0.05, and false discovery rate < 0.00003. Boldface type indicates genes involved in fluid absorption or surfactant protein/phospholipid synthesis, trafficking, or reutilization.

* Denotes mRNA expression previously detected in whole lung or lung cells.

† Denotes mRNA expression previously localized to alveolar type II cells.

‡ Molecular functions were derived from the Gene Ontology Consortium, and additional annotations are in parentheses.

pathologic and histologic levels. Photographs of lungs from mice exposed to nickel for 48 and 72 h and nonexposed control animals are shown in Figures 3A–3C. As acute lung injury progressed, the lung surface appeared red in color, indicative of hemorrhage and coagulation. Histologic analysis of lung sections from nickel-exposed mice as compared with control animals revealed progressive pulmonary edema marked by perivascular swelling and interstitial thickening (Figures 3D–3I).

The increased expression of genes involved in fibrinolysis as measured by microarray are presented in Figure 4A. RT-PCR confirmed SERPINE1 transcript levels increased at 24, 48, and 72 h (Figure 4B). These RT-PCR data support increased gene expression observed by microarray (Table 2).

Effect of TGF-β Inhibition *In Vivo*

Total BAL protein (measured at 72 h after the initiation of exposure to nickel) was significantly lower in 129S1/SvImJ mice administered murine soluble chimeric TGFβRII-Fc just before and 6 and 30 h after a 24-h exposure to nickel as compared with saline-injected mice (Figure 5). Both TGFβRII-Fc– and saline-treated mice had significantly greater BAL protein after nickel exposure compared with saline-treated nonexposed control animals. Total cells, neutrophils, and macrophages in BAL were not different between all treatment/exposure groups (Table 4).

TGF-β Represses *Sftpb* Transcription in Mouse Lung Epithelial Cells

Previously, we reported that *Sftpb* gene expression decreases in lungs of mice exposed to nickel (17). MLE-15 cells transfected with the –653/+35 (wild-type) promoter construct were treated with increasing doses of TGF-β1 (0.1–30 ng/ml) for 24 h to determine the effect of TGF-β on *Sftpb* transcription. Luciferase activities (normalized to β-galactosidase) of the –653/+35 (wild-type) promoter were significantly decreased below untreated (control) values in a dose-dependent manner after treatment with TGF-β1 (Figure 6A). This is consistent with previously

TABLE 2. SIGNIFICANTLY INCREASED GENES DETERMINED BY OLIGONUCLEOTIDE MICROARRAY ANALYSIS IN 129S1/SVIMJ MOUSE LUNGS AFTER EXPOSURE TO NICKEL FOR 24, 48, OR 72 H

Accession ID	Name	Symbol	Intensity	24 h	SEM	48 h	SEM	72 h	SEM	Molecular Function†
K02236	Metallothionein 2*	Mt2	991	15.4	4.0	16.9	4.3	33.6	8.6	Metal ion binding
V00755	**Tissue inhibitor of metalloproteinase 1***	**Timp1**	**930**	**10.5**	**3.0**	**18.0**	**5.6**	**25.5**	**7.7**	**Metalloendopeptidase inhibitor activity**
NM_011580	**Thrombospondin 1***	**Thbs1**	**1036**	**7.5**	**3.2**	**10.6**	**4.9**	**20.2**	**7.9**	**Structural molecule activity**
M83219	**S100 calcium binding protein A9 (calgranulin B)***	**S100a9**	**389**	**2.5**	**0.9**	**5.3**	**1.8**	**17.4**	**6.0**	**Calcium ion binding**
NM_011607	**Tenascin C***	**Tnc**	**300**	**4.4**	**1.6**	**6.6**	**2.3**	**15.1**	**5.3**	**Protein binding**
M19681	Chemokine (C-C motif) ligand 2*	Ccl2	300	4.5	2.2	7.7	4.9	12.8	6.3	Chemokine activity
AF057156	Small proline-rich protein 1A*	Sprr1a	415	32.7	13.9	19.5	10.8	11.5	4.9	Structural molecule activity
AF058798	Stratifin	Sfn	483	9.9	2.4	8.1	2.2	9.6	2.3	Protein domain-specific binding
X81627	Lipocalin 2*	Lcn2	801	2.6	0.9	3.6	1.2	8.6	3.0	Transporter activity
NM_009263	**Secreted phosphoprotein 1***	**Spp1**	**305**	**3.7**	**0.9**	**2.7**	**0.6**	**8.0**	**1.9**	**Protein binding**
Z29532	**Follistatin***	**Fst**	**374**	**3.5**	**0.8**	**7.6**	**1.8**	**7.2**	**1.7**	**Activin inhibitor activity**
AF205951	Resistin-like α*	Retnla	5300	15.9	4.0	8.4	2.1	7.1	1.8	Hormone activity
X61597	Serine (or cysteine) proteinase inhibitor, clade A, member 3C*	Serpina3c	489	3.1	0.8	5.2	1.3	7.0	1.7	Serine-type endopeptidase inhibitor activity
AK007630	Cyclin-dependent kinase inhibitor 1A (P21)*	Cdkn1a	1112	6.7	2.1	4.7	1.4	6.2	1.9	Cyclin-dependent protein kinase inhibitor activity
NM_013749	Tumor necrosis factor receptor superfamily, member 12a*	Tnfrsf12a	592	2.8	0.6	2.8	0.6	5.9	1.1	Receptor activity
Y08222	Forkhead box C2*	Foxc2	454	1.5	0.4	1.6	0.4	5.6	1.5	Transcription factor activity
U85498	Glutamate-cysteine ligase, catalytic subunit*	Gclc	1098	6.2	1.3	5.0	1.0	5.4	1.1	Glutamate-cysteine ligase activity
M23384	Solute carrier family 2 (facilitated glucose transporter), member 1*	Slc2a1	486	6.9	1.8	3.2	0.9	5.1	1.3	Glucose transporter activity
M27960	Interleukin 4 receptor, α*	Il4ra	585	2.8	0.8	4.1	1.1	5.0	1.4	Interleukin receptor activity
J03520	**Plasminogen activator, tissue***	**Plat**	**347**	**2.0**	**0.5**	**3.1**	**0.7**	**4.9**	**1.2**	**Serine-type endopeptidase activity**
AB025408	Esterase D/formylglutathione hydrolase	Esd	715	3.1	0.6	3.8	0.7	4.8	0.9	Serine esterase activity
AF171100	LPS-induced tumor necrosis factor*	Litaf	697	2.8	0.4	3.1	0.4	4.7	0.8	Transcription factor activity
NM_023119	**Enolase 1, α nonneuron***	**Eno1**	**1685**	**10.4**	**2.9**	**6.7**	**1.8**	**4.5**	**1.2**	**Phosphopyruvate hydratase activity**
M65027	Glycoprotein 49 A*	Gp49a	415	2.2	0.6	3.6	1.0	4.4	1.1	(Immunoglobin-like receptor activity)
M33960	**Serine (or cysteine) proteinase inhibitor, clade E, member 1***	**Serpine1**	**313**	**6.6**	**2.5**	**4.9**	**2.7**	**4.4**	**1.8**	**Serine-type endopeptidase inhibitor activity**
M15668	**Phosphoglycerate kinase 1***	**Pgk1**	**975**	**7.3**	**1.2**	**6.0**	**1.0**	**4.3**	**0.7**	**Phosphoglycerate kinase activity**
U19604	Ligase I, DNA, ATP-dependent*	Lig1	309	1.4	0.3	2.6	0.5	4.3	0.9	DNA ligase (ATP) activity
NM_010171	**Coagulation factor III***	**F3**	**1046**	**4.1**	**0.8**	**3.9**	**0.8**	**4.2**	**0.8**	**Blood coagulation/receptor activity**
U05265	Glycoprotein 49B*	Gp49b	448	2.3	0.6	4.0	1.3	4.2	1.2	(Immunoglobin-like inhibitory receptor activity)
AB007696	Prostaglandin E receptor 2 (subtype EP2)*	Ptger2	313	3.5	1.0	3.5	1.2	4.0	1.0	Prostaglandin E activity
U08210	**Elastin***	**Eln**	**665**	**1.5**	**0.4**	**2.0**	**0.5**	**3.6**	**0.8**	**Extracellular matrix structural constituent**
U54984	**Matrix metalloproteinase 14 (membrane-inserted)***	**Mmp14**	**762**	**1.3**	**0.2**	**1.5**	**0.3**	**3.3**	**0.6**	**Metalloendopeptidase activity**

Values shown for each time point are mean fold changes over nonexposed control values. Genes are sorted by 72-h mean value and were considered statistically significant if intensity > 300, $p < 0.5 \times 10^{-6}$, expected false-positive < 0.05, and false discovery rate < 0.00003. Boldface indicates genes involved in transforming growth factor-β signaling and plasminogen activation.

* Denotes mRNA expression previously detected in whole lung or lung cells.

† Molecular functions were derived from the Gene Ontology Consortium, and additional annotations are in parentheses.

noted repression of human SFTPB by TGF-β *in vitro* (26, 27). In addition, the effect of TGF-β1 on the repression of *Sftpb* transcription was reversed in cells transfected with the Δ(−616/−198) construct treated with 30 ng/ml TGF-β1 (Figure 6B). Luciferase activity of the –653/+35 (wild-type; 43% of the nonexposed control value) was significantly decreased below that of the Δ(−616/−198) construct (69% of the nonexposed control value) after 30 ng/ml TGF-β1 treatment. These data suggest that *cis*-acting elements between –616 to –198 in the *Sftpb* promoter are partially responsible for its repression by TGF-β1.

DISCUSSION

Microarray Analyses

In the present study, molecular events of acute lung injury were identified using oligonucleotide microarray analysis to examine temporal transcript changes in the lungs of 129S1/SvImJ mice after exposure to nickel. The first level of analysis of the microarray data was a statistical analysis of genes that were significantly different from controls. This information was the starting point from which subsequent analyses were performed, and served as a foundation for investigations of the underlying biological pathways that control responses to inhaled nickel. Transcriptional analyses, however, are not trouble-free and can suffer from limitations. Microarray results are typically expressed as a fold increase or decrease. Although useful, without a context it may be difficult to ascribe biological meaning to this outcome measure. For example, large fold increases (i.e., 10- to 100-fold) may solely reflect tissue-specific (an absence of constitutive) expression in control tissue.

In the initial analysis of the microarray data, many of the genes that were decreased the most after 72 h of exposure to

TABLE 3. IDENTIFICATION OF SIGNIFICANTLY CHANGED MOLECULAR PATHWAYS BY MAPPFINDER ANALYSIS OF AN OLIGONUCLEOTIDE MICROARRAY DATASET FROM LUNGS OF 129S1/SVIMJ MICE EXPOSED TO NICKEL FOR 72 H

Pathway Name/GO Term	Genes Changed	Genes Measured	z Score
Extracellular matrix	36	94	3.7
Cysteine protease inhibitor	5	6	3.5
TGF-β signaling pathway	10	21	2.8
Cytokine	20	53	2.8
Pancreatic RNase	4	6	2.5
Protein kinase A anchor protein	3	4	2.5
Protein-lysine 6-oxidase	3	4	2.5
Heparin binding	7	14	2.4
Chemokine	9	20	2.3
Growth factor binding	4	6	2.3
Insulinlike growth factor binding	5	9	2.3
Growth factor	19	51	2.2
Copper binding	4	7	2.1
Toxin	3	4	2.1
Chaperone	12	26	2.1

Definition of abbreviations: GO = Gene Ontology; TGF = transforming growth factor.

MAPPFinder calculates a cumulative total of genes changed for a parent GO term and its children and provides a statistical z score to assess significance; z score values greater than 2.0 were considered to be significant.

nickel play important roles in lung fluid absorption or surfactant and phospholipid synthesis (Table 1). Perturbation of these physiologic processes contributes to the development of acute lung injury. For example, *Atp1b1* expression was notably decreased in our model of acute lung injury. *Atp1b1* is a key element in the regulation of active Na^+ transport in alveolar epithelium that keeps the airspaces free of excess fluid (28–30), which is a hallmark of patients with acute lung injury (31).

Genes involved in surfactant and phospholipid production, metabolism, and trafficking were also among those that were most significantly decreased. For instance, *Pltp* assists in the uptake of secreted surfactant lipids, and plays a role in surfactant lipid trafficking and reutilization in alveolar type II epithelial cells (32). *Slc34a2* is a transporter that recycles intracellular phosphate, an essential component for surfactant phospholipid synthesis (33). Fatty acids are important constituents of surfactant, and can also alter surfactant synthesis. *Fasn* and *Scd2* were significantly decreased by nickel exposure and function in the generation of fatty acid in alveolar epithelial cells (34). In addition, *Napsa* is involved in the proper processing of surfactant-associated protein B (35), and knockdown of *Napsa* in type II cells results in decreased levels of the mature SP (36). Taken together, these data and our previous data on decreased *Sftpb* expression in nickel-induced acute lung injury indicate that the transcript levels of several essential genes in the synthesis and function of pulmonary surfactant are significantly decreased, and these expression changes may cumulatively lead to surfactant disruption in nickel-induced acute lung injury.

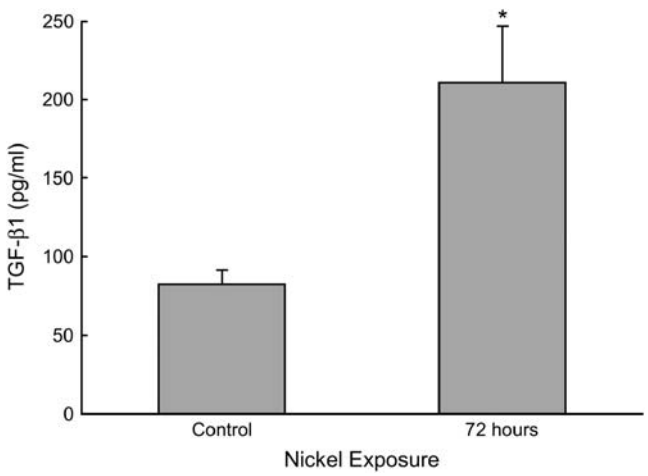

Figure 1. Increased transforming growth factor (TGF)-β protein in lungs of mice exposed to nickel for 72 h. TGF-β1 in bronchoalveolar lavage fluid (BALF) was measured by ELISA. Data are presented as means ± SEM (n = 5 mice/group). * Denotes significant difference from nonexposed control group, $p < 0.05$.

MAPPFinder was used to further analyze the functional pathways altered by nickel exposure by performing pathway-based analysis of the microarray data. A major benefit of this type of analysis is that it generates a description of the biology that is occurring within the dataset, in contrast to hierarchic clustering or self-organizing maps that arrange genes according to similarity in pattern of gene expression (17, 37, 38). Pathways that had a large number of expression changes include extracellular matrix, cytokine, and chemokine. In another microarray analysis of TGF-β signaling, Verrecchia and colleagues (39) identified genes (including *TIMP1*, *THBS1*, *PAI-1*, *TNC*, and *MMP14*) rapidly induced by TGF-β in human dermal fibroblasts. Similarly, many of the identified genes (67% of those measured in both experiments) exhibited altered expression in mice with acute lung injury. Furthermore, MAPPFinder established that TGF-β signaling was significantly altered in our mouse model, which supported the changes in genes of the TGF-β signaling pathway in the initial analysis of the genes most increased in our microarray data (Table 2), and suggested that TGF-β was a central mediator of nickel-induced acute lung injury.

Modulation of Extracellular Matrix and Fibrinolysis by TGF-β

TGF-β activation is known to play a role in the development of acute lung injury in humans and laboratory animals through alteration of fibroproliferative responses, lung permeability, and inflammatory cell influx (7, 12, 40, 41). However, the molecular mechanisms of TGF-β in acute lung injury are not well understood. Our data suggest that increased TGF-β altered multiple lung cell functions important to the initiation and progression of acute lung injury. The careful use of gene expression microarray analysis identified specific molecular alterations underlying the functional changes.

We found that TGF-β1 protein increased in BAL after exposure to nickel. The extracellular concentration of TGF-β protein is mainly controlled by the conversion of inactive TGF-β (secreted as inactive complexes containing TGF-β, the TGF-β propeptide, and latent TGF-β binding protein) to active TGF-β. Activated TGF-β is then able to induce lung cells to generate more total TGF-β via autoinduction. There are two distinct potential mechanisms by which TGF-β could be activated in our system. First, integrin αvβ6 is an *in vivo* activator of latent TGF-β1 through the recognition of an arginine-glycine-aspartic acid site on the TGF-β propeptide (42, 43). Second, activation of latent TGF-β can be achieved by direct binding of thrombospondin 1 protein (44, 45). Transcripts for ITGAV and THBS1 were significantly increased after nickel exposure.

Increased TGF-β levels are able induce *Spp1* (46), *Timp1* (47, 48), and *Tnc* (49) gene expression. SPP1 is a matricellular protein that possesses cytokine-like properties and can act as a chemoattractant for macrophages (50, 51). SPP1 also regulates fibrogenic signals in epithelial repair after bleomycin-induced

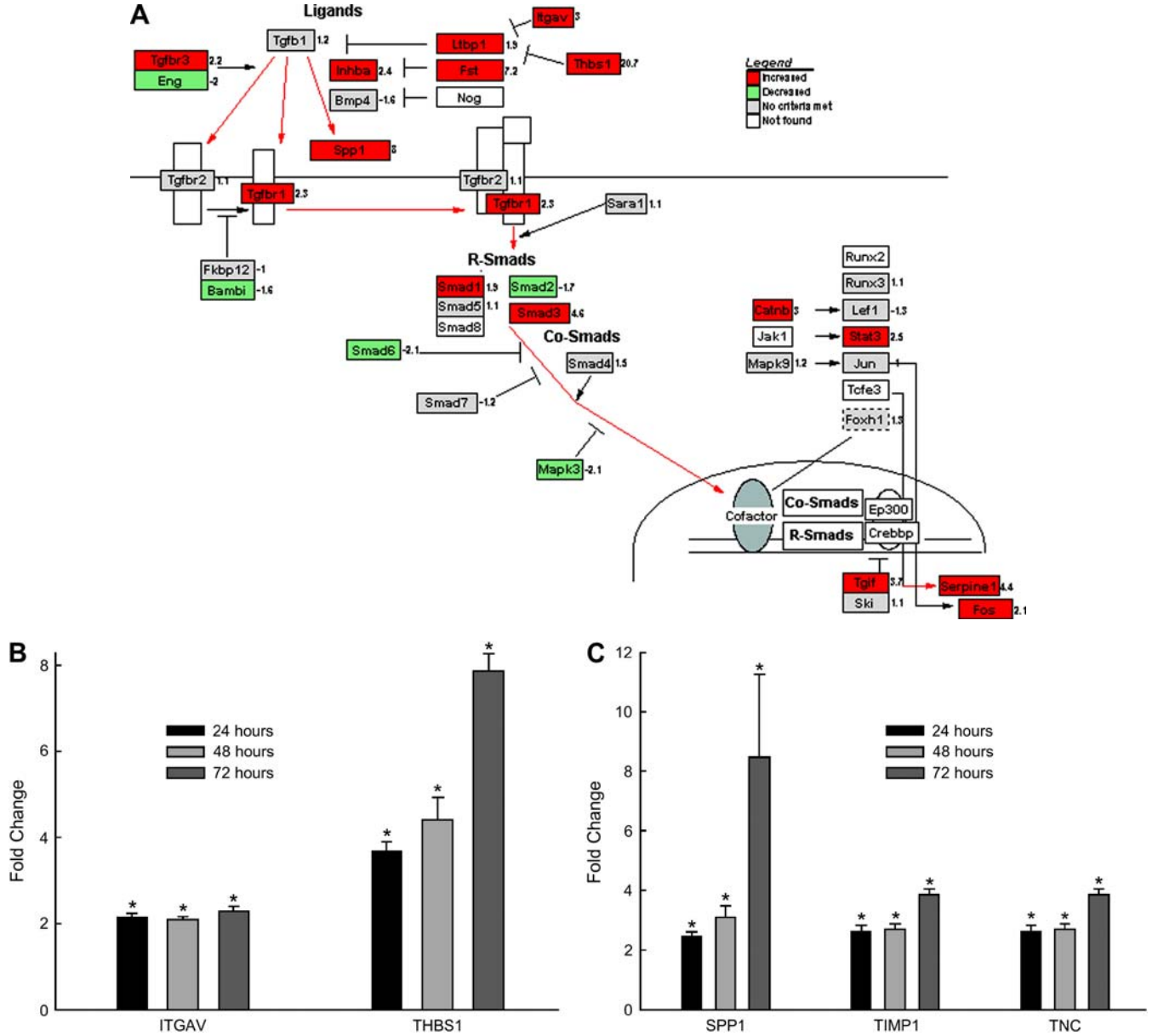

Figure 2. Expression changes in genes of the TGF-β signaling pathway in lungs of mice exposed to nickel as measured by oligonucleotide microarray and reverse transcriptase–polymerase chain reaction (RT-PCR). (*A*) Changes in gene expression are expressed using the GenMAPP format. Genes that were increased atleast 1.5-fold over control values and had a significance value of $p \leqslant 0.05$ are labeled in *red*. Those genes that were decreased atleast 1.5-fold from control values and had a significance value of $p \leqslant 0.05$ are labeled in *green*. Those genes that did not meet the aforementioned criteria are labeled in *gray*, and those genes that were not on the array are labeled in *white*. (*B*) RT-PCR analysis of mRNA for genes that are activators of TGF-β after 24, 48, or 72 h of exposure. Data are presented as fold changes over control values (n = 5 mice/group, means ± SEM) and are normalized to ribosomal protein S2 (*Rps2*) expression. * Denotes significant difference from nonexposed control group, $p < 0.05$. ITGAV = integrin αV; THBS1 = thrombospondin 1. (C) RT-PCR analysis of mRNA for genes that are activated by TGF-β after 24, 48, or 72 h of exposure. Data are presented as fold changes over control values (n = 5 mice/group, means ± SEM) and are normalized to *Rps2* expression. * Denotes significant difference from nonexposed control group, $p < 0.05$. SPP1 = secreted phosphoprotein 1; TIMP1 = tissue inhibitor of metalloproteinase 1; TNC = tenascin C.

lung injury (52). TIMP1 is a metalloproteinase inhibitor that can mediate inflammation and repair processes during acute lung injury through stabilization of matrix components (53). TNC is an extracellular matrix glycoprotein that may play a role similar to TIMP1 (54, 55). Interestingly, SPP1 (56) and TNC (57) contain an arginine-glycine-aspartic amino acid sequence that could activate TGF-β in a positive feedback loop involving integrins (58). The expression of *Spp1*, *Timp1*, and *Tnc* was markedly increased after 72 h of nickel exposure, suggesting that the activation of the TGF-β pathway has an effect on the expression of extracellular matrix–altering genes in our model of acute lung injury.

Coagulation and fibrinolysis are processes that form and dissolve fibrin, respectively. These processes are precisely regulated and serve to protect from excessive blood loss or undue fibrin deposition. Moreover, acute and chronic pulmonary diseases are characterized by impaired fibrinolytic activity within the lung

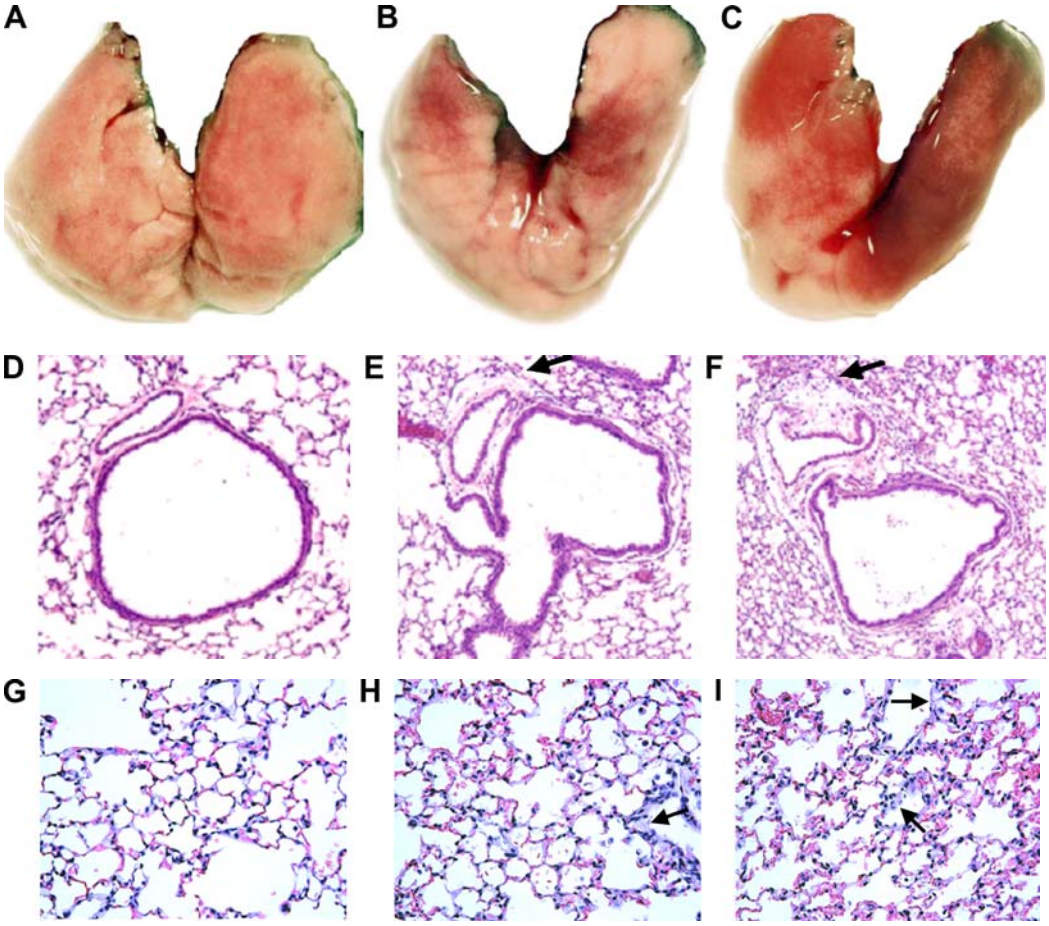

Figure 3. Gross pathology (*A*–*C*) and light microscope histology (*D*–*I*) of lungs of mice exposed to nickel for 48 and 72 h, and nonexposed control animals. (*A*) Nonexposed control lung, (*B*) 48-h exposed lung, (*C*) 72-h exposed lung, (*D*) non-exposed control (original magnification × 40), (*E*) 48-h exposed (original magnification × 40), (*F*) 72-h exposed (original magnification × 40), (*G*) nonexposed control (original magnification × 400), (*H*) 48-h exposed (original magnification × 400), (*I*) 72-h exposed (original magnification × 400). The gross pathologic progression of acute lung injury is apparent, with the lung surface appearing in *red* from hemorrhage and coagulation as exposure progressed as compared with nonexposed control lungs (*A*–*C*). Histologic analysis of lung sections from nickel-exposed mice compared with control animals showed a progressive increase in perivascular swelling (*arrows*, *E* and *F*) and alveolar wall thickening (*arrows*, *H* and *I*).

(59, 60). Increased lung TGF-β may play a role in the modulation of fibrinolysis through the induction of *Serpine1* in our model of acute lung injury. *PAI-1* (known as *Serpine1* in mice) is the major inhibitor of fibrinolytic activity in the alveolar space (59), and is highly induced by TGF-β (61). Previous studies by Andrew and coworkers (62, 63) have demonstrated that nickel is also able to transcriptionally induce *PAI-1* and inhibit fibrinolytic activity in human airway epithelial cells (64). Transcript levels of SERPINE1 were significantly increased after nickel exposure (Figure 4), and pathologic and histologic analyses of the exposed mouse lungs confirmed alterations in fibrinolysis.

Attenuation of Nickel-induced BAL Protein by TGFβRII-Fc *In Vivo*

Studies investigating the role of TGF-β in lung injury have focused mainly on its function in the mediation of fibroproliferation and resolution of tissue injury. Inhibition of TGF-β by a monoclonal antibody hindered the induction of proinflammatory cytokines and lung injury induced by hemorrhagic shock (65). More recently, Pitett and colleagues (12) found that administration of the soluble TGFβRII-Fc chimera was an effective inhibitor of integrin αvβ6–mediated activation of TGF-β, and also inhibits many TGF-β–mediated processes *in vitro* and *in vivo* (66, 67). Moreover, these investigators have demonstrated that integrin αvβ6–mediated local activation of TGF-β is important in the development of bleomycin-induced pulmonary edema using integrin $\beta6^{-/-}$ mice. In this study, treatment of integrin $\beta6^{+/+}$ wild-type mice (129/terSVEMS strain) with TGFβRII-Fc prevented increased lung permeability as assessed approximately 120 h after instillation of bleomycin or *Escherichia coli* endotoxin (12). These observations agree with our data in which administration of soluble TGFβRII-Fc chimera attenuated nickel-induced BAL protein measured at 72 h after the initiation of nickel exposure. The attenuation of permeability we observed was less than that of Pittet and coworkers, which may be due to differences in the agonist (nickel vs. bleomycin vs. *E. coli* endotoxin) or the magnitude of injury. Moreover, TGF-β has been found to decrease sodium channel–dependent fluid transport (13–15), and decreases in ATP1B1 and SCNN1B transcript levels noted here may have contributed to edema. Inhibition of TGF-β did not lessen BAL neutrophils and macrophages after nickel exposure, which is also consistent with Pitett and colleagues' findings with bleomycin-treated integrin $\beta6^{-/-}$ mice. Taken together, these findings support an important role for TGF-β activation in the development of lung hyperpermeability and edema in acute lung injury.

Modulation of *Sftpb* Promoter Activity by TGF-β *In Vitro*

We have previously demonstrated that exposure to nickel decreases lung *Sftpb* gene expression in a time-dependent fashion in mice (17). The increase in TGF-β in the lungs of mice after nickel exposure may have contributed to the decrease in *Sftpb* expression. Using a human fetal lung explant model, TGF-β inhibited *Sftpb* expression and protein synthesis (26, 68). In the present study, treatment with TGF-β1 dose-dependently repressed –653/+35 (wild-type) *Sftpb* promoter construct activity in MLE-15 (Figure 5A). Furthermore, the Δ(−616/−198) construct exhibited an attenuation of TGF-β1 repression of *Sftpb*

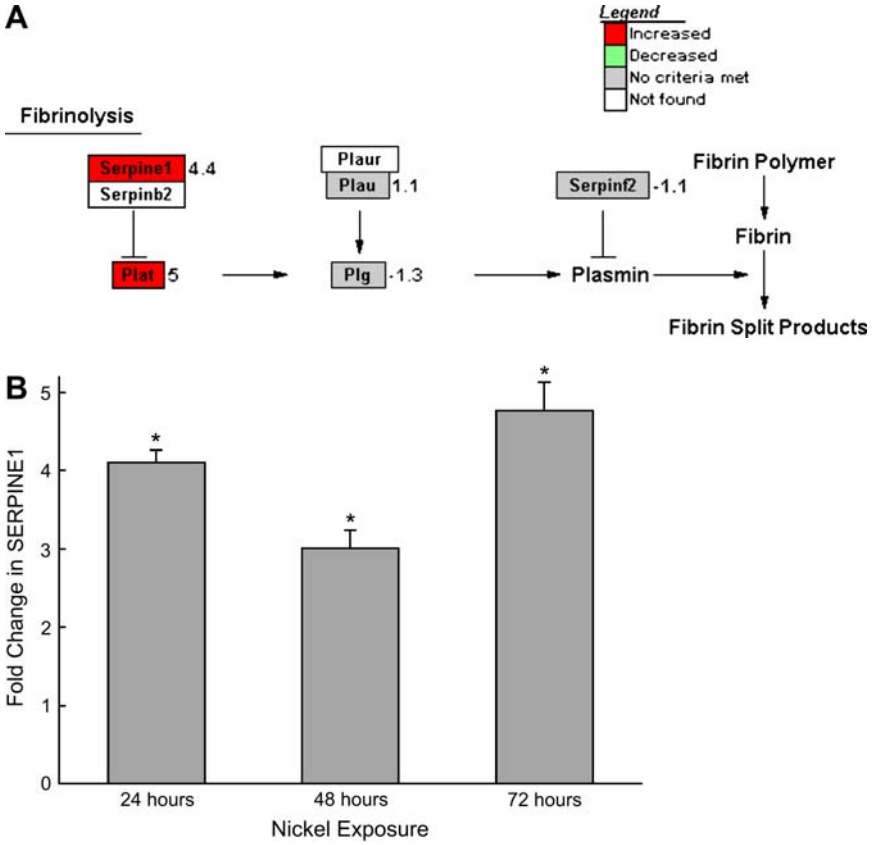

Figure 4. Expression changes in genes of the fibrinolysis signaling pathway in lungs of mice exposed to nickel for 72 h as measured by oligonucleotide microarray and RT-PCR. (*A*) Changes in gene expression are expressed using the GenMAPP format. Genes that were increased at least 1.5-fold over control values and had a significance value of $p \leq 0.05$ are labeled in *red*. Those genes that were decreased at least 1.5-fold from control values and had a significance value of $p \leq 0.05$ are labeled in *green*. Those genes that did not meet the aforementioned criteria are labeled in *gray*, and those genes that were not on the array are labeled in *white*. (*B*) RT-PCR analysis of serine (or cysteine) proteinase inhibitor, clade E, member 1 (Serpine1) mRNA after 24, 48, or 72 h of exposure. Data are presented as fold changes over control values (n = 5 mice/group, means ± SEM) and are normalized to *Rps2* expression. * Denotes significant difference from nonexposed control group, $p < 0.05$.

activity, providing evidence for a putative TGF-β1–responsive *cis*-acting repressor element(s) between –653 to –198 in the mouse *Sftpb* promoter. The lack of *Sftpb* repression by TGF-β1 with the Δ(−616/−198) construct is in contrast to a study by Kumar and coworkers (69) in which repression was observed in a similar human *SFTPB* construct that was used in National Cancer Institute H441 lung tumor cells. The dissimilarities between these data could be due to the collective differences in the reporter constructs used, the transfection conditions, the duration of TGF-β1 exposure, and the cell types used in the experiments.

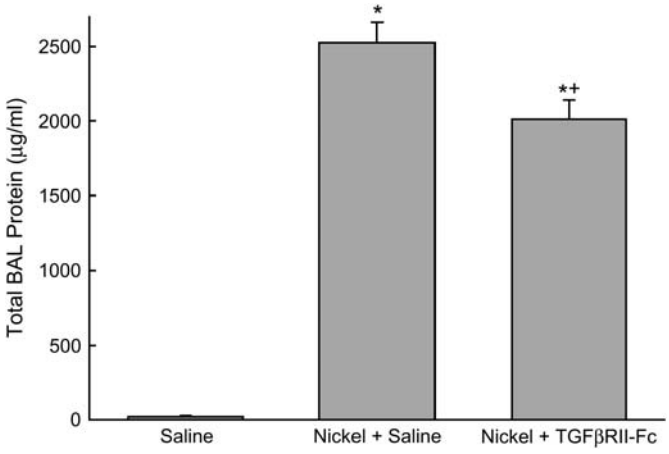

Figure 5. Soluble chimeric TGF-β type II receptor (TGFβRII-Fc) attenuates nickel-induced BAL protein in 129S1/SvImJ mice. Mice were intravenously administered TGFβRII-Fc (50 μg in 50 μl sterile saline) or saline alone immediately before and 6 and 30 h after a 24-h exposure to nickel. Nonexposed control mice were also concurrently injected with saline. All mice were lavaged 72 h after the initiation of nickel-exposure. Data are presented as means ± SEM. * Denotes significant difference from nonexposed saline-treated control group, $p < 0.05$; $^{+}$denotes significant difference from nickel-exposed saline-treated group, $p < 0.05$.

Transcriptional regulation by TGF-β is regulated by a family of factors known as mothers against decapentaplegic homologs (SMAD), which act as intracellular effectors of TGF-β signaling (70). One mechanism of TGF-β inhibition of human *SFTPB* was found to be through SMAD3 protein–protein interactions with thyroid transcription factor-1 (TITF1) and hepatocyte nuclear factor transcription factors in H441 cells (27). TGF-β–mediated gene expression changes can also occur via direct binding of SMAD proteins to promoter "CAGA" elements in target genes (71–74). In the –653/+35 (wild-type) promoter used in the present study, there are four CAGA motifs located between –653 to –198 that could be involved in SMAD-mediated TGF-β inhibition of *Sftpb*.

Several additional transcription factor binding sites are located between –653 to –198 that could be involved in TGF-β inhibition of *Sftpb*, including one activator protein (AP)-1 site, one nuclear factor (NF)-κB site, two NFI sites, and one TITF1 site. AP-1 binding sites in the promoters of several genes have been functionally associated with transcriptional regulation by TGF-β (13, 75–77), and SMAD proteins act synergistically with AP-1 complexes in TGF-β–responsive genes (78–81). Transcriptional regulation of the mouse *Sftpb* promoter can be regulated by AP-1 family members (82). Alterations in gene expression by TGF-β can also be transcriptionally regulated by NF-κB (83). In addition, SMAD and NFI DNA binding domains are similar

TABLE 4. TOTAL CELLS, NEUTROPHILS, AND MACROPHAGES RECOVERED IN BRONCHOALVEOLAR LAVAGE FLUID FROM 129S1/SVIMJ MICE ADMINISTERED SALINE OR TGFβRII-FC AND EXPOSED TO NICKEL OR NONEXPOSED CONTROL ANIMALS

	Total Cells ($\times 10^4$)	Neutrophils ($\times 10^4$)	Macrophages ($\times 10^4$)
Saline, nonexposed	8.8 ± 3.9	0.05 ± 0.03	8.7 ± 3.8
Nickel + saline	7.1 ± 0.8	2.5 ± 0.8*	4.6 ± 1.1
Nickel + TGFβRII-Fc	12.2 ± 2.4	3.0 ± 0.9*	9.1 ± 1.7

Definition of abbreviation: TGFβRII-Fc = transforming growth factor-β type II receptor–IgG-Fc.

Values are means ± SEM; n = 5 mice/group. Murine soluble chimeric TGFβRII-Fc or saline alone was intravenously administered immediately before and 6 and 30 h after a 24-h exposure to nickel. Nonexposed control mice were concurrently injected with saline. All mice were lavaged 72 h after the initiation of nickel exposure.

* Denotes significantly different from saline-injected nonexposed control animals ($p < 0.05$).

(84), and NFI and TITF-1 have been shown to modulate surfactant-associated protein C transcription (85). Further investigation is necessary to elucidate the transcriptional mechanism of TGF-β suppression of *Sftpb* in our *in vitro* model.

The probable role of TGF-β in our model of acute lung injury is schematically presented in Figure 7. Identification of the genes that changed the most using high stringencies for significance demonstrated that many genes that are involved in proper surfactant synthesis and trafficking and fluid absorption were significantly decreased, and several genes that are associated with the TGF-β pathway were significantly increased. MAPPFinder analysis indicated that TGF-β signaling is significantly altered in lungs of mice after exposure to nickel. Activation of TGF-β can then regulate critical downstream events in the development of acute lung injury, such as extracellular matrix gene expression, fibrinolysis (through *Serpine1*), and *Sftpb* expression. Inhibition of TGF-β with soluble chimeric TGFβRII-Fc attenuated nickel-induced protein in BAL. Transient transfection assays with mouse *Sftpb* promoter constructs demonstrated that TGF-β plays an important role in the regulation of *Sftpb* transcription in mouse lung epithelial cells. Due to the complex nature of the molecular mechanisms of acute lung injury and the innate limitations of any mouse model of disease, the implications of our results to acute lung injury in humans is an important question. In

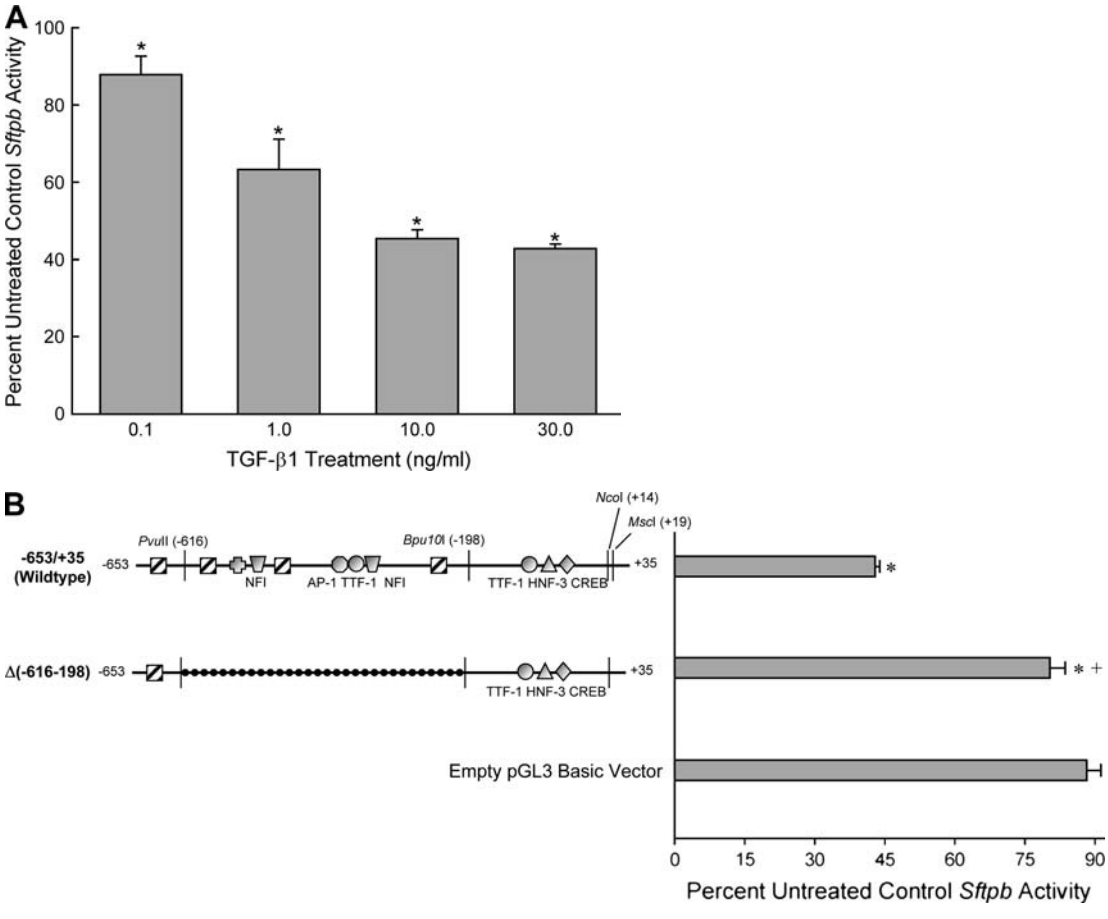

Figure 6. Repression of *Sftpb* promoter activity by TGF-β1 *in vitro*. (*A*) Transient transfections of the –653/+35 (wild-type) mouse *Sftpb* luciferase promoter construct were done in MLE-15 cells (750 ng of construct/well and 250 ng of cytomegalovirus promoter–β-galactosidase/well as an internal control) and treated with 0.1, 1.0, 10, and 30 ng/ml TGF-β1 for 24 h. (*B*) Transient transfections of the –653/+35 (wild-type) and Δ(−616/−198) mouse *Sftpb* luciferase promoter constructs were done in MLE-15 cells (750 ng of construct/well and 250 ng of pCMV–β-galactosidase/well as an internal control) and treated with 30 ng/ml TGF-β1 for 24 h. For both *panels*, relative luciferase activities normalized to cotransfected β-galactosidase are expressed as percentage of untreated control values. Values are means ± SEM (n = 5–11/group). * Denotes significant difference from untreated control, $p < 0.05$; $^+$ denotes significant difference from –653/+35 (wild-type) *Sftpb* promoter construct, $p < 0.05$. *Striped boxes* denote location of "CAGA" elements. Other promoter elements are as labeled in the figure. CREB = cydic adenosine monophosphate (CAMP)–responsive element-binding protein; HNF-3 = hepatocyte nuclear factor 3; TTF-1 = thyroid transcription factor 1.

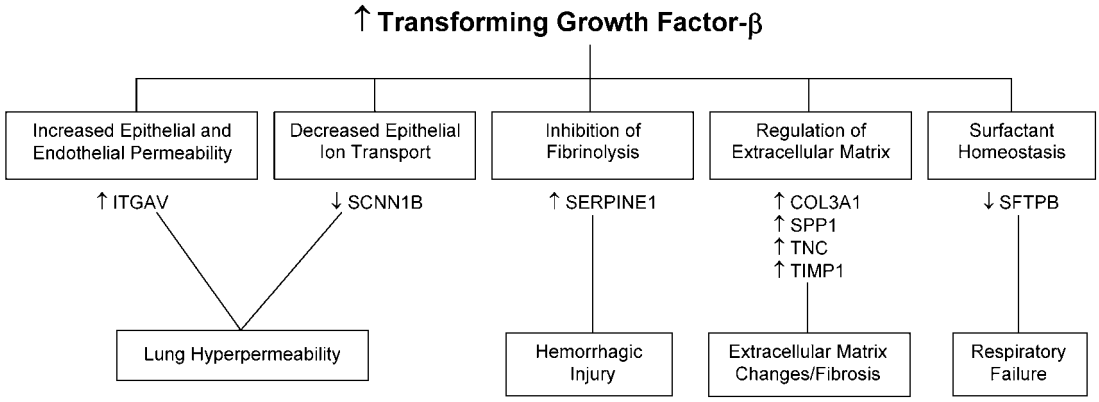

Figure 7. Schematic diagram of the role of TGF-β in acute lung injury. After exposure to nickel, TGF-β is increased in the lungs of mice. TGF-β and TGF-β–inducible genes are able to modify lung permeability, epithelial ion transport, fibrinolysis, the extracellular matrix, and surfactant homeostasis. The integration of the changes in these molecular pathways by TGF-β implicates it as a central mediator of acute lung injury.

addition, we do not know how TGF-β may be functioning at much earlier time points in our model of acute lung injury. However, our findings suggest that TGF-β may act as a central mediator in the development of acute lung injury, and reinforce previous studies that have implicated TGF-β in other models of acute lung injury. These data should stimulate further investigations on the role of TGF-β in acute lung injury, novel therapeutic tactics, and additional mechanisms by which intersecting molecular pathways are able to regulate the pathogenesis of acute lung injury.

Conflict of Interest Statement: None of the authors have a financial relationship with a commercial entity that has an interest in the subject of this manuscript.

Acknowledgment: The authors thank Cindy J. Bachurski (Cincinnati Children's Hospital Medical Center) for the plasmid gift and Dean Sheppard (University of California–San Francisco) for critical reading of this manuscript.

References

1. Ware LB, Matthay MA. The acute respiratory distress syndrome. *N Engl J Med* 2000;342:1334–1349.
2. Lewis JF, Jobe AH. Surfactant and the adult respiratory distress syndrome. *Am Rev Respir Dis* 1993;147:218–233.
3. Grande JP. Role of transforming growth factor-beta in tissue injury and repair. *Proc Soc Exp Biol Med* 1997;214:27–40.
4. Singer AJ, Clark RA. Cutaneous wound healing. *N Engl J Med* 1999; 341:738–746.
5. Broekelmann TJ, Limper AH, Colby TV, McDonald JA. Transforming growth factor beta 1 is present at sites of extracellular matrix gene expression in human pulmonary fibrosis. *Proc Natl Acad Sci USA* 1991;88:6642–6646.
6. Giri SN, Hyde DM, Hollinger MA. Effect of antibody to transforming growth factor beta on bleomycin induced accumulation of lung collagen in mice. *Thorax* 1993;48:959–966.
7. Fahy RJ, Lichtenberger F, McKeegan CB, Nuovo GJ, Marsh CB, Wewers MD. The acute respiratory distress syndrome: a role for transforming growth factor-beta 1. *Am J Respir Cell Mol Biol* 2003;28:499–503.
8. Chesnutt AN, Matthay MA, Tibayan FA, Clark JG. Early detection of type III procollagen peptide in acute lung injury: pathogenetic and prognostic significance. *Am J Respir Crit Care Med* 1997;156:840–845.
9. Clark JG, Milberg JA, Steinberg KP, Hudson LD. Type III procollagen peptide in the adult respiratory distress syndrome: association of increased peptide levels in bronchoalveolar lavage fluid with increased risk for death. *Ann Intern Med* 1995;122:17–23.
10. Kaminski N, Allard JD, Pittet JF, Zuo F, Griffiths MJ, Morris D, Huang X, Sheppard D, Heller RA. Global analysis of gene expression in pulmonary fibrosis reveals distinct programs regulating lung inflammation and fibrosis. *Proc Natl Acad Sci USA* 2000;97:1778–1783.
11. Hurst VI, Goldberg PL, Minnear FL, Heimark RL, Vincent PA. Rearrangement of adherens junctions by transforming growth factor-beta1: role of contraction. *Am J Physiol Lung Cell Mol Physiol* 1999; 276:L582–L595.
12. Pittet JF, Griffiths MJ, Geiser T, Kaminski N, Dalton SL, Huang X, Brown LA, Gotwals PJ, Koteliansky VE, Matthay MA, *et al.* TGF-beta is a critical mediator of acute lung injury. *J Clin Invest* 2001; 107:1537–1544.
13. Frank J, Roux J, Kawakatsu H, Su G, Dagenais A, Berthiaume Y, Howard M, Canessa CM, Fang X, Sheppard D, *et al.* Transforming growth factor-beta1 decreases expression of the epithelial sodium channel alphaENaC and alveolar epithelial vectorial sodium and fluid transport via an ERK1/2-dependent mechanism. *J Biol Chem* 2003;278:43939–43950.
14. Willis BC, Kim KJ, Li X, Liebler J, Crandall ED, Borok Z. Modulation of ion conductance and active transport by TGF-beta 1 in alveolar epithelial cell monolayers. *Am J Physiol Lung Cell Mol Physiol* 2003; 285:L1192–L1200.
15. Roux J, Kawakatsu H, Gartland B, Pespeni M, Sheppard D, Matthay MA, Canessa CM, Pittet JF. Interleukin-1beta decreases expression of the epithelial sodium channel alpha-subunit in alveolar epithelial cells via a p38 MAPK-dependent signaling pathway. *J Biol Chem* 2005;280:18579–18589.
16. Wesselkamper SC, Prows DR, Biswas P, Willeke K, Bingham E, Leikauf GD. Genetic susceptibility to irritant-induced acute lung injury in mice. *Am J Physiol Lung Cell Mol Physiol* 2000;279:L575–L582.
17. McDowell SA, Gammon K, Bachurski CJ, Wiest JS, Leikauf JE, Prows DR, Leikauf GD. Differential gene expression in the initiation and progression of nickel-induced acute lung injury. *Am J Respir Cell Mol Biol* 2000;23:466–474.
18. Prows DR, Leikauf GD. Quantitative trait analysis of nickel-induced acute lung injury in mice. *Am J Respir Cell Mol Biol* 2001;24:740–746.
19. Doniger SW, Salomonis N, Dahlquist KD, Vranizan K, Lawlor SC, Conklin BR. MAPPFinder: using Gene Ontology and GenMAPP to create a global gene-expression profile from microarray data. *Genome Biol* 2003;4:R7.
20. Karyala S, Guo J, Sartor M, Medvedovic M, Kann S, Puga A, Ryan P, Tomlinson CR. Different global gene expression profiles in benzo[a]-pyrene- and dioxin-treated vascular smooth muscle cells of AHR-knockout and wild-type mice. *Cardiovasc Toxicol* 2004;4:47–73.
21. Saltini C, Hance AJ, Ferrans VJ, Basset F, Bitterman PB, Crystal RG. Accurate quantification of cells recovered by bronchoalveolar lavage. *Am Rev Respir Dis* 1984;130:650–658.
22. Wikenheiser KA, Vorbroker DK, Rice WR, Clark JC, Bachurski CJ, Oie HK, Whitsett JA. Production of immortalized distal respiratory epithelial cell lines from surfactant protein C/simian virus 40 large tumor antigen transgenic mice. *Proc Natl Acad Sci USA* 1993;90: 11029–11033.
23. Wolfinger RD, Gibson G, Wolfinger ED, Bennett L, Hamadeh H, Bushel P, Afshari C, Paules RS. Assessing gene significance from cDNA microarray expression data via mixed models. *J Comput Biol* 2001; 8:625–637.
24. Benjamini Y, Hochberg Y. Controlling the false discovery rate: a practical and powerful approach to multiple testing. *J R Stat Soc (Ser A)* 1995; B57:289–300.
25. Dahlquist KD, Salomonis N, Vranizan K, Lawlor SC, Conklin BR. GenMAPP, a new tool for viewing and analyzing microarray data on biological pathways. *Nat Genet* 2002;31:19–20.

26. Whitsett JA, Weaver TE, Lieberman MA, Clark JC, Daugherty C. Differential effects of epidermal growth factor and transforming growth factor-beta on synthesis of Mr = 35,000 surfactant-associated protein in fetal lung. *J Biol Chem* 1987;262:7908–7913.
27. Li C, Zhu NL, Tan RC, Ballard PL, Derynck R, Minoo P. Transforming growth factor-beta inhibits pulmonary surfactant protein B gene transcription through SMAD3 interactions with NKX2.1 and HNF-3 transcription factors. *J Biol Chem* 2002;277:38399–38408.
28. Factor P, Dumasius V, Saldias F, Brown LA, Sznajder JI. Adenovirus-mediated transfer of an Na+/K+-ATPase beta1 subunit gene improves alveolar fluid clearance and survival in hyperoxic rats. *Hum Gene Ther* 2000;11:2231–2242.
29. Adir Y, Factor P, Dumasius V, Ridge KM, Sznajder JI. Na,K-ATPase gene transfer increases liquid clearance during ventilation-induced lung injury. *Am J Respir Crit Care Med* 2003;168:1445–1448.
30. Machado-Aranda D, Adir Y, Young JL, Briva A, Budinger GR, Yeldandi AV, Sznajder JI, Dean DA. Gene transfer of the Na+,K+-ATPase beta1 subunit using electroporation increases lung liquid clearance. *Am J Respir Crit Care Med* 2005;171:204–211.
31. Ware LB, Matthay MA. Alveolar fluid clearance is impaired in the majority of patients with acute lung injury and the acute respiratory distress syndrome. *Am J Respir Crit Care Med* 2001;163:1376–1383.
32. Jiang XC, D'Armiento J, Mallampalli RK, Mar J, Yan SF, Lin M. Expression of plasma phospholipid transfer protein mRNA in normal and emphysematous lungs and regulation by hypoxia. *J Biol Chem* 1998; 273:15714–15718.
33. Traebert M, Hattenhauer O, Murer H, Kaissling B, Biber J. Expression of type II Na-P(i) cotransporter in alveolar type II cells. *Am J Physiol Lung Cell Mol Physiol* 1999;277:L868–L873.
34. Zhang F, Pan T, Nielsen LD, Mason RJ. Lipogenesis in fetal rat lung: importance of C/EBPalpha, SREBP-1c, and stearoyl-CoA desaturase. *Am J Respir Cell Mol Biol* 2004;30:174–183.
35. Brasch F, Ochs M, Kahne T, Guttentag S, Schauer-Vukasinovic V, Derrick M, Johnen G, Kapp N, Muller KM, Richter J, *et al.* Involvement of napsin A in the C- and N-terminal processing of surfactant protein B in type-II pneumocytes of the human lung. *J Biol Chem* 2003;278: 49006–49014.
36. Ueno T, Linder S, Na CL, Rice WR, Johansson J, Weaver TE. Processing of pulmonary surfactant protein B by napsin and cathepsin H. *J Biol Chem* 2004;279:16178–16184.
37. Eisen MB, Spellman PT, Brown PO, Botstein D. Cluster analysis and display of genome-wide expression patterns. *Proc Natl Acad Sci USA* 1998;95:14863–14868.
38. Tamayo P, Slonim D, Mesirov J, Zhu Q, Kitareewan S, Dmitrovsky E, Lander ES, Golub TR. Interpreting patterns of gene expression with self-organizing maps: methods and application to hematopoietic differentiation. *Proc Natl Acad Sci USA* 1999;96:2907–2912.
39. Verrecchia F, Chu ML, Mauviel A. Identification of novel TGF-beta /Smad gene targets in dermal fibroblasts using a combined cDNA microarray/promoter transactivation approach. *J Biol Chem* 2001; 276:17058–17062.
40. Cui X, Zeni F, Vodovitz Y, Correa-de-Araujo R, Quezado M, Roberts A, Wahl S, Danner RL, Banks SM, Gerstenberger E, *et al.* TGF-beta1 increases microbial clearance but worsens lung injury during Escherichia coli pneumonia in rats. *Cytokine* 2003;24:115–127.
41. Bechara RI, Brown LA, Roman J, Joshi PC, Guidot DM. Transforming growth factor β1 expression and activation is increased in the alcoholic rat lung. *Am J Respir Crit Care Med* 2004;170:188–194.
42. Munger JS, Huang X, Kawakatsu H, Griffiths MJ, Dalton SL, Wu J, Pittet JF, Kaminski N, Garat C, Matthay MA, *et al.* The integrin alpha v beta 6 binds and activates latent TGF beta 1: a mechanism for regulating pulmonary inflammation and fibrosis. *Cell* 1999;96:319–328.
43. Annes JP, Chen Y, Munger JS, Rifkin DB. Integrin alphaVbeta6-mediated activation of latent TGF-beta requires the latent TGF-beta binding protein-1. *J Cell Biol* 2004;165:723–734.
44. Schultz-Cherry S, Chen H, Mosher DF, Misenheimer TM, Krutzsch HC, Roberts DD, Murphy-Ullrich JE. Regulation of transforming growth factor-beta activation by discrete sequences of thrombospondin 1. *J Biol Chem* 1995;270:7304–7310.
45. Crawford SE, Stellmach V, Murphy-Ullrich JE, Ribeiro SM, Lawler J, Hynes RO, Boivin GP, Bouck N. Thrombospondin-1 is a major activator of TGF-beta1 in vivo. *Cell* 1998;93:1159–1170.
46. Shi X, Bai S, Li L, Cao X. Hoxa-9 represses transforming growth factor-beta-induced osteopontin gene transcription. *J Biol Chem* 2001;276: 850–855.
47. Edwards DR, Murphy G, Reynolds JJ, Whitham SE, Docherty AJ, Angel P, Heath JK. Transforming growth factor beta modulates the expression of collagenase and metalloproteinase inhibitor. *EMBO J* 1987; 6:1899–1904.
48. Hall MC, Young DA, Waters JG, Rowan AD, Chantry A, Edwards DR, Clark IM. The comparative role of activator protein 1 and Smad factors in the regulation of Timp-1 and MMP-1 gene expression by transforming growth factor-beta 1. *J Biol Chem* 2003;278:10304–10313.
49. Jinnin M, Ihn H, Asano Y, Yamane K, Trojanowska M, Tamaki K. Tenascin-C upregulation by transforming growth factor-beta in human dermal fibroblasts involves Smad3, Sp1, and Ets1. *Oncogene* 2004; 23:1656–1667.
50. Ophascharoensuk V, Giachelli CM, Gordon K, Hughes J, Pichler R, Brown P, Liaw L, Schmidt R, Shankland SJ, Alpers CE, *et al.* Obstructive uropathy in the mouse: role of osteopontin in interstitial fibrosis and apoptosis. *Kidney Int* 1999;56:571–580.
51. O'Regan AW, Hayden JM, Body S, Liaw L, Mulligan N, Goetschkes M, Berman JS. Abnormal pulmonary granuloma formation in osteopontin-deficient mice. *Am J Respir Crit Care Med* 2001;164:2243–2247.
52. Berman JS, Serlin D, Li X, Whitley G, Hayes J, Rishikof DC, Ricupero DA, Liaw L, Goetschkes M, O'Regan AW. Altered bleomycin-induced lung fibrosis in osteopontin-deficient mice. *Am J Physiol Lung Cell Mol Physiol* 2004;286:L1311–L1318.
53. Madtes DK, Elston AL, Kaback LA, Clark JG. Selective induction of tissue inhibitor of metalloproteinase-1 in bleomycin-induced pulmonary fibrosis. *Am J Respir Cell Mol Biol* 2001;24:599–607.
54. Zhao Y, Young SL, McIntosh JC. Induction of tenascin in rat lungs undergoing bleomycin-induced pulmonary fibrosis. *Am J Physiol Lung Cell Mol Physiol* 1998;274:L1049–L1057.
55. Kaarteenaho-Wiik R, Kinnula VL, Herva R, Soini Y, Pollanen R, Paakko P. Tenascin-C is highly expressed in respiratory distress syndrome and bronchopulmonary dysplasia. *J Histochem Cytochem* 2002; 50:423–431.
56. Ruoslahti E, Pierschbacher MD. New perspectives in cell adhesion: RGD and integrins. *Science* 1987;238:491–497.
57. Leahy DJ, Hendrickson WA, Aukhil I, Erickson HP. Structure of a fibronectin type III domain from tenascin phased by MAD analysis of the selenomethionyl protein. *Science* 1992;258:987–991.
58. Ortega-Velazquez R, Diez-Marques ML, Ruiz-Torres MP, Gonzalez-Rubio M, Rodriguez-Puyol M, Rodriguez Puyol D. Arg-Gly-Asp-Ser (RGDS) peptide stimulates transforming growth factor beta1 transcription and secretion through integrin activation. *FASEB J* 2003; 17:1529–1531.
59. Idell S, Peters J, James KK, Fair DS, Coalson JJ. Local abnormalities of coagulation and fibrinolytic pathways that promote alveolar fibrin deposition in the lungs of baboons with diffuse alveolar damage. *J Clin Invest* 1989;84:181–193.
60. Eitzman DT, McCoy RD, Zheng X, Fay WP, Shen T, Ginsburg D, Simon RH. Bleomycin-induced pulmonary fibrosis in transgenic mice that either lack or overexpress the murine plasminogen activator inhibitor-1 gene. *J Clin Invest* 1996;97:232–237.
61. Boehm JR, Kutz SM, Sage EH, Staiano-Coico L, Higgins PJ. Growth state-dependent regulation of plasminogen activator inhibitor type-1 gene expression during epithelial cell stimulation by serum and transforming growth factor-beta1. *J Cell Physiol* 1999;181:96–106.
62. Andrew AS, Klei LR, Barchowsky A. Nickel requires hypoxia-inducible factor-1 alpha, not redox signaling, to induce plasminogen activator inhibitor-1. *Am J Physiol Lung Cell Mol Physiol* 2001;281:L607–L615.
63. Andrew AS, Klei LR, Barchowsky A. AP-1-dependent induction of plasminogen activator inhibitor-1 by nickel does not require reactive oxygen. *Am J Physiol Lung Cell Mol Physiol* 2001;281:L616–L623.
64. Andrew A, Barchowsky A. Nickel-induced plasminogen activator inhibitor-1 expression inhibits the fibrinolytic activity of human airway epithelial cells. *Toxicol Appl Pharmacol* 2000;168:50–57.
65. Shenkar R, Coulson WF, Abraham E. Anti-transforming growth factor-beta monoclonal antibodies prevent lung injury in hemorrhaged mice. *Am J Respir Cell Mol Biol* 1994;11:351–357.
66. Wang Q, Wang Y, Hyde DM, Gotwals PJ, Koteliansky VE, Ryan ST, Giri SN. Reduction of bleomycin induced lung fibrosis by transforming growth factor beta soluble receptor in hamsters. *Thorax* 1999;54:805–812.
67. Smith JD, Bryant SR, Couper LL, Vary CP, Gotwals PJ, Koteliansky VE, Lindner V. Soluble transforming growth factor-beta type II receptor inhibits negative remodeling, fibroblast transdifferentiation, and intimal lesion formation but not endothelial growth. *Circ Res* 1999;84: 1212–1222.
68. Beers MF, Solarin KO, Guttentag SH, Rosenbloom J, Kormilli A, Gonzales LW, Ballard PL. TGF-beta1 inhibits surfactant component expression and epithelial cell maturation in cultured human fetal lung. *Am J Physiol Lung Cell Mol Physiol* 1998;275:L950–L960.

69. Kumar AS, Gonzales LW, Ballard PL. Transforming growth factor-beta(1) regulation of surfactant protein B gene expression is mediated by protein kinase-dependent intracellular translocation of thyroid transcription factor-1 and hepatocyte nuclear factor 3. *Biochim Biophys Acta* 2000;1492:45–55.
70. Heldin CH, Miyazono K, ten Dijke P. TGF-beta signalling from cell membrane to nucleus through SMAD proteins. *Nature* 1997;390:465–471.
71. Dennler S, Itoh S, Vivien D, ten Dijke P, Huet S, Gauthier JM. Direct binding of Smad3 and Smad4 to critical TGF beta-inducible elements in the promoter of human plasminogen activator inhibitor-type 1 gene. *EMBO J* 1998;17:3091–3100.
72. Chen SJ, Yuan W, Lo S, Trojanowska M, Varga J. Interaction of smad3 with a proximal smad-binding element of the human alpha2(I) procollagen gene promoter required for transcriptional activation by TGF-beta. *J Cell Physiol* 2000;183:381–392.
73. Poncelet AC, Schnaper HW. Sp1 and Smad proteins cooperate to mediate transforming growth factor-beta 1-induced alpha 2(I) collagen expression in human glomerular mesangial cells. *J Biol Chem* 2001;276:6983–6992.
74. Puente E, Saint-Laurent N, Torrisani J, Furet C, Schally AV, Vaysse N, Buscail L, Susini C. Transcriptional activation of mouse sst2 somatostatin receptor promoter by transforming growth factor-beta. Involvement of Smad4. *J Biol Chem* 2001;276:13461–13468.
75. Chung KY, Agarwal A, Uitto J, Mauviel A. An AP-1 binding sequence is essential for regulation of the human alpha2(I) collagen (COL1A2) promoter activity by transforming growth factor-beta. *J Biol Chem* 1996;271:3272–3278.
76. Keeton MR, Curriden SA, van Zonneveld AJ, Loskutoff DJ. Identification of regulatory sequences in the type 1 plasminogen activator inhibitor gene responsive to transforming growth factor beta. *J Biol Chem* 1991;266:23048–23052.
77. Tang W, Yang L, Yang YC, Leng SX, Elias JA. Transforming growth factor-beta stimulates interleukin-11 transcription via complex activating protein-1-dependent pathways. *J Biol Chem* 1998;273:5506–5513.
78. Zhang Y, Feng XH, Derynck R. Smad3 and Smad4 cooperate with c-Jun/c-Fos to mediate TGF-beta-induced transcription. *Nature* 1998;394:909–913.
79. Wong C, Rougier-Chapman EM, Frederick JP, Datto MB, Liberati NT, Li JM, Wang XF. Smad3-Smad4 and AP-1 complexes synergize in transcriptional activation of the c-Jun promoter by transforming growth factor beta. *Mol Cell Biol* 1999;19:1821–1830.
80. Qing J, Zhang Y, Derynck R. Structural and functional characterization of the transforming growth factor-beta -induced Smad3/c-Jun transcriptional cooperativity. *J Biol Chem* 2000;275:38802–38812.
81. Yamamura Y, Hua X, Bergelson S, Lodish HF. Critical role of Smads and AP-1 complex in transforming growth factor-beta-dependent apoptosis. *J Biol Chem* 2000;275:36295–36302.
82. Sever-Chroneos Z, Bachurski CJ, Yan C, Whitsett JA. Regulation of mouse SP-B gene promoter by AP-1 family members. *Am J Physiol Lung Cell Mol Physiol* 1999;277:L79–L88.
83. Ogawa K, Chen F, Kuang C, Chen Y. Suppression of matrix metalloproteinase-9 transcription by transforming growth factor-beta is mediated by a nuclear factor-kappaB site. *Biochem J* 2004;381:413–422.
84. Stefancsik R, Sarkar S. Relationship between the DNA binding domains of SMAD and NFI/CTF transcription factors defines a new superfamily of genes. *DNA Seq* 2003;14:233–239.
85. Bachurski CJ, Yang GH, Currier TA, Gronostajski RM, Hong D. Nuclear factor I/thyroid transcription factor 1 interactions modulate surfactant protein C transcription. *Mol Cell Biol* 2003;23:9014–9024.